Applied Ergonomics 44 (2013) 841–849

Contents lists available at SciVerse ScienceDirect

Applied Ergonomics

journal homepage: www.elsevier.com/locate/apergo

Biomechanical loading of the shoulder complex and lumbosacral joints during dynamic cart pushing task

Ashish D. Nimbarte [a,*], Yun Sun [b], Majid Jaridi [a], Hongwei Hsiao [c]

[a] Department of Industrial and Management Systems Engineering, PO Box 6070, West Virginia University, Morgantown, WV 26506-6107, USA
[b] Safety Studies, Keene State College, 229 Main Street, Keene, NH 03435-1901, USA
[c] National Institute for Occupational Safety and Health, 1095 Willowdale Road, Morgantown, WV 26505, USA

ARTICLE INFO

Article history:
Received 14 August 2012
Accepted 14 February 2013

Keywords:
Cart
Pushing
Shoulder
Low back
Biomechanical loading

ABSTRACT

The primary objective of this study was to quantify the effect of dynamic cart pushing exertions on the biomechanical loading of shoulder and low back. Ten participants performed cart pushing tasks on flat (0°), 5°, and 10° ramped walkways at 20 kg, 30 kg, and 40 kg weight conditions. An optoelectronic motion capturing system configured with two force plates was used for the kinematic and ground reaction force data collection. The experimental data was modeled using AnyBody modeling system to compute three-dimensional peak reaction forces at the shoulder complex (sternoclavicular, acromioclavicular, and glenohumeral) and low back (lumbosacral) joints. The main effect of walkway gradient and cart weight, and gradient by weight interaction on the biomechanical loading of shoulder complex and low back joints was statistically significant (all $p < 0.001$). At the lumbosacral joint, negligible loading in the mediolateral direction was observed compared to the anterioposterior and compression directions. Among the shoulder complex joints, the peak reaction forces at the acromioclavicular and glenohumeral joints were comparable and much higher than the sternoclavicular joint. Increased shear loading of the lumbosacral joint, distraction loading of glenohumeral joint and inferosuperior loading of the acromioclavicular joint may contribute to the risk of work-related low back and shoulder musculoskeletal disorder with prolonged and repetitive use of carts.

1. Introduction

The overall burden of work-related musculoskeletal disorders (WMSDs) is enormous in terms of corporate economics and individual health. In the United States, the cost of WMSDs associated with workers' compensation, lost wages, and decreased productivity ranges between $45 and $54 billion annually (Dunning et al., 2010). In 2010, WMSDs among occupational groups such as laborers and material movers, heavy and tractor-trailer truck drivers, and delivery service truck drivers, whose routine work demands manual material handling (MMH) tasks, constitute 12% of all WMSD cases (144,910 out of 1,238,490 cases) requiring days away from work (Bureau of Labor Statistics, 2010).

Manual material handling (MMH) tasks typically consist of activities such as lifting/lowering, pushing/pulling, and holding/carrying loads (Smith et al., 2009; Snook, 1978). In recent years, with the advent of e-commerce, the number of distribution centers has increased world-wide. The primary jobs of the workers at these distribution centers involve order picking and delivery, which typically are performed using manual handling aids such as carts, trolleys, and hand-pallet trucks on level and ramped surfaces. The use of such assist devices eliminates manual carrying and in some cases lifting and lowering, changing the nature of MMH tasks predominantly to pushing and pulling. It has been estimated that nearly half of MMH tasks common at workplaces consist of pushing and pulling exertions performed on level surfaces and variable inclined ramps (Lee and Granata, 2006).

Despite the increased occurrence of pushing and pulling tasks performed using manual assist devices in occupational settings, the effect of such exertions on the quantitative loading of the musculoskeletal system was seldom studied. Such knowledge is essential to understand the etiology of musculoskeletal complaints associated with the pushing and pulling exertions. Schibye et al. (2001) evaluated musculoskeletal loading of the low back during pushing and pulling exertions performed by refuse collection workers using a two-wheeled hand cart with 25 kg and 50 kg weights. Peak L4/L5 compression and shear loading of up to 1500 N and 200 N, respectively was estimated by the authors using a quasi-static two

* Corresponding author. Tel.: +1 304 293 9473; fax: +1 304 293 4970.
E-mail addresses: Ashish.Nimbarte@mail.wvu.edu, nimbarte.ashish@gmail.com (A.D. Nimbarte), ysun@keene.edu (Y. Sun), Majid.Jaridi@mail.wvu.edu (M. Jaridi), hxh4@cdc.gov (H. Hsiao).

0003-6870/$ – see front matter © 2013 Elsevier Ltd and The Ergonomics Society. All rights reserved.
http://dx.doi.org/10.1016/j.apergo.2013.02.008

dimensional link segment model. Jäger et al. (2007) reported peak L5/S1 compression and shear loading of up to 2200 N and 200 N, respectively, for flight attendants' four-wheeled cart pushing and pulling tasks performed under three weight conditions (40 kg, 65 kg, and 95 kg). In this study, a spatial dynamic multi-segmental biomechanical model was applied quasi-statically to estimate musculoskeletal loading. Using an electromyography (EMG) assisted optimization model, that accounted for the muscle co-contraction, Hoozemans et al. (2004) estimated peak L5/S1 compression and shear forces of up to 1521 N and 485 N, respectively, during a four wheeled cart pushing tasks (weights = 85, 135 and 320 kg). By applying a similar method, Knapik and Marras (2009) estimated peak L5/S1 compression and anterioposterior shear forces of up to 1500 N and 500 N, respectively; pushing pulling forces of 20%, 30% and 40% of body weight were used in this study.

The compression and shear loadings reported in the aforementioned dynamic pushing and pulling studies are well below the critical loading limits of 3400 N (Waters et al., 1993) and 500 N (McGill, 2007), respectively. This suggests minimal risk of low back WMSDs. However, in spite of a known association between shoulder WMSDs and work-related pushing exertions (Hoozemans et al., 2002a, b; Hoozemans et al., 1998; Hughes et al., 1997; Smedley et al., 2003; van der Beek et al., 1993; van der Beek et al., 1999), the effect of such exertions on the biomechanical loading of shoulder joints is currently not well understood. Therefore, in this study a comprehensive full-body musculoskeletal model was used to evaluate the effect of pushing exertions performed using manual carts on the shoulder and low back joints. The specific study objectives were: (1) formulate a biomechanical model to access dynamic pushing tasks; (2) validate the model; (3) quantify effect of cart weight and walkway gradients on the loading of shoulder complex and low back joints using this model. Three walkway gradients (0°, 5° and 10°) and 3 weights (20, 30 and 40 kg) were tested in this study.

2. Material and methods

2.1. Approach

A laboratory-based study was performed to quantify the effect of dynamic two-wheeled cart pushing tasks on the biomechanical loading of the shoulder complex and low back joints. Human participants performed the pushing tasks at different cart weight and walkway gradient conditions. Three-dimensional (3D) kinematic and ground reaction force data were recorded using an eight camera marker-based optoelectronic motion analysis system coupled with two ground reaction force plates. The experimental data were modeled using a full-body musculoskeletal model to compute the biomechanical loading of the shoulder complex and low back joints. The model outputs for cart wheel reaction force were validated by comparing it with experimentally measured vertical ground reaction forces.

2.2. Participants

Ten male participants were recruited for data collection. Their average age, weight, and height were 23.8 (1.8) years, 69.2 (5.0) kg, and 172.0 (4.3) cm, respectively. All participants were free of acute and chronic back, shoulder, or other upper extremity MSDs and had no known neurological disorders. The Physical Activity Readiness Questionnaire (PAR-Q, British Columbia Ministry of Health) was used to screen participants for cardiac and other health problems (e.g., dizziness, chest pain, and heart trouble).

2.3. Apparatus

2.3.1. Motion-capture system

An optoelectronic motion-capture system (Vicon Motion Systems, CA, USA) was used for recording 3D kinematic data. This system consists of eight optical cameras that emit infrared light which reflects off of small retro-reflective markers. The cameras capture the reflected light and record the location of the markers in 3D space. The marker data were processed using Vicon Nexus 1.5.1 Software (Vicon Motion Systems, CA, USA). This software allows further processing of marker data (e.g., labeling, gap filling, filtering) to compute marker coordinates in 3D space. Marker data was sampled at a rate of 100 Hz.

2.3.2. Custom made walkway

A walkway measuring 0.9 m (3 feet) wide and 6 m (20 feet) long was constructed using a reinforced wooden frame with cut-outs for two force plates. Two Kistler force plates (type 9286, Kistler Instrument Corp., Amherst, NY, USA) were embedded in the wooden walkway to record the ground reaction force (GRF) data (Fig. 1(a)). A hydraulic scissor lift table (EHLT-4872-3-43, Vestil Manufacturing Corp., IN, USA) was attached to one end of the wooden walkway using a hinge assembly. This table has a collapsed height of 0.18 m (7 inches) and can be raised to a maximum height of 0.91 m (36 inches). When completely collapsed, the lift table and walkway provide a flat walking surface. To set up different walkway gradients, the table height was raised using a hydraulic actuator.

2.3.3. Two-wheeled hand cart

A two-wheeled Harper hand cart (CSLEDTK1935P, Harper Trucks, Inc., Wichita, KS, USA) was used. This hand cart (1.25 m height × 0.31 m depth × 0.33 m width) weighs 12 kg and has a capacity of 317 kg (700 lbs). The height of the handle is 1.25 m above ground level with the cart in an upright position and about 0.85 m in a tilted position ready to be moved. Each wheel, made of rubber, is a 10-inch pneumatic tire. The coefficient of friction for the cart wheels on a wooden walkway was reported to be approximately 1.3 by the manufacturer.

2.4. Description of the model

The cart pushing model was developed using the AnyBody musculoskeletal simulation software (version 4.0, AnyBody Technology, Aalborg, Denmark). This software combines a solver for the multi-body inverse dynamics problem with optimizers that address and solve the redundancy of the muscle recruitment problem (Damsgaard et al., 2006; Dubowsky et al., 2008). Gait full body model in the public domain AnyScript Model Repository (AnyBody Technology, 2011) was used as the base-model to develop the cart pushing model. The gait full body includes a total of 34 rigid bodies, 33 joints and over 750 muscle fascicles with real physiological properties. The model environment, which contains objects surrounding the human model, was modified by adding a cart segment (Fig. 2). This segment was defined as a rigid body, formed using eighteen nodes joined together using a polyline object (AnyBody Modeling System, 2012). Additionally, two nodes for the right and left handle were created to connect the cart with the hands. The mass properties of the cart were defined by means of a mass and an inertia tensor.

2.5. Experimental data collection

Upon arriving at the laboratory, participants were provided with a tour of the experimental set-up. Equipment, data collection procedures, and specifics of the experimental tasks were explained to

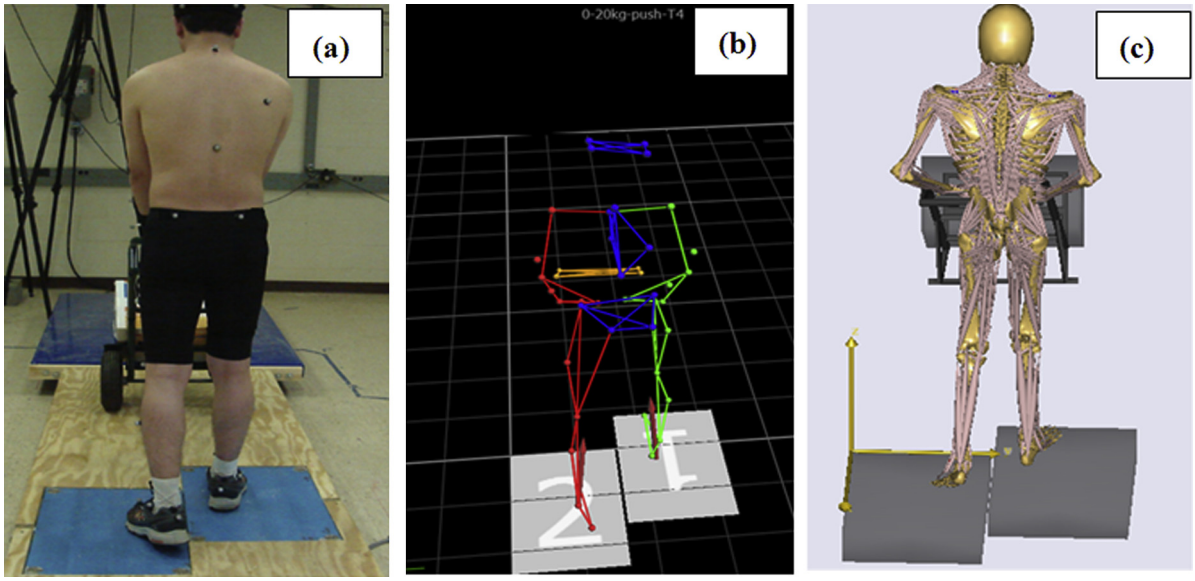

Fig. 1. (a) A participant performing cart pushing task on a flat walkway; (b) Corresponding marker data labeled using Vicon Nexus software to generate C3D data file; (c) The biomechanical model driven using the C3D data in the AnyBody modeling system.

the participants and their signatures were obtained on the consent form approved by the local Institutional Review Board. Demographics and anthropometric measures were then recorded for each participant.

The participants then changed into a test shirt and pant and a set of thirty-nine reflective markers (diameter = 0.025 m) were affixed on the various anatomical locations based on the Vicon Plug-in-Gait marker set (Vicon Plug in Gait Manual, 2003). Additionally four markers were placed on the cart to track its motion during the pushing tasks. Participants were subsequently instructed to perform the pushing tasks using their natural gait and self-selected technique. All of the participants practiced the pushing tasks on different gradients at least three times to get themselves familiarized with the nature of physical exertion.

Following the above preparatory steps, participants performed the dynamic cart pushing tasks on three walkway gradients (0°, 5° and 10°) using 3 weights (20, 30 and 40 kg). While specific data on the ramp inclinations used in the industrial setting is not available, OSHA recommends that a ramp angle greater than 20° from the horizontal must be provided with handrails, and ramps exceeding 30° from the horizontal would be prohibited (OSHA, 2005). In the previous studied ramps of 0°, 2°, 5°, 8°, and 12° were tested (Bennett et al., 2008; Glitsch et al., 2007; Jäger et al., 2007). The two gradients of 0° and 5° were selected to be comparable with the previous studies, while the third gradient of 10° was determined based on the capture volume restriction of the optical motion analysis system used in this study. Most of the participants had extreme difficulty pushing weight greater than 40 kg on the 10° walkway, therefore three weights of 20 kg (low), 30 kg (medium) and 40 kg (high) were selected in this study. In the preliminary data collection, the duration of an individual trial was approximately 30–45 s with a rest period of 90–120 s between the trials. Three replicates were collected and the trial order was randomized.

Fig. 2. A cart pushing model developed using AnyBody modeling system.

2.6. Data processing

Marker and GRF data were processed using Vicon Nexus software and exported in the C3D format. The data transition involved in these processing steps is illustrated in Fig. 1. The 3D marker trajectories and GRF data were used as the model input. Marker trajectories were used to drive the cart pushing model. The following steps were involved in running the modeling analysis:

(1) Scaling the model based on the participants' anthropometry
(2) Optimizing model parameters such as marker location, segment lengths, and joint locations using 3D marker kinematics.
(3) Performing inverse dynamics analysis to compute muscle and joint forces.

In the AnyBody Modeling System, the muscle force required to generate motion or sustain body posture is computed using inverse-dynamic methods by solving a multi-body dynamics problem. The muscle recruitment in the inverse dynamics process is solved using a min/max optimization procedure (Rasmussen

et al., 2001), within which the objective function is to minimize the maximal normalized muscle force. The objective function of the optimization procedure is:

$$G\left(f^{(M)}\right) = \max\left(\frac{f_i^{(M)}}{N_i}\right)$$

Subjected to the following constraints:

$$Cf = d$$

$$\left(f_i^{(M)}\right) \geq 0; i \in \{1, \ldots, n^{(M)}\}$$

Where, **f** is the vector of $n^{(M)}$ unknown muscle forces, $\mathbf{f}^{(M)}$, and joint reactions, $\mathbf{f}^{(R)}$. *Ni* is the momentary strength of muscle *i*. *C* is the coefficient matrix for the "unknown" forces/moments in the system while *d* is a vector of the "known" (applied or inertia) forces.

The lower bound ($f_i^{(M)} > 0$) simply states that muscles can only pull (not push) and that the upper bound for the force in each muscle *i* is the corresponding muscle strength, *Ni*;

The model output consists of various muscle and joint reaction forces. In this study, reaction forces in three anatomical directions (compression or inferosuperior, mediolateral or distraction, and anterioposterior) for the following shoulder complex and low back joints were derived for further analysis:

(1) Sternoclavicular joint
(2) Acromioclavicular joint
(3) Glenohumeral joint
(4) Lumbosacral (L5/S1) joint

2.7. Model validation

AnyBody human models were previously validated in a number of studies (de Zee and Rasmussen, 2009; Dubowsky et al., 2008; Manders et al., 2008; Rasmussen et al., 2007) and were successfully used to estimate muscle and joint reaction forces for various occupational scenarios (Grujicic et al., 2010; Wu et al., 2008, 2009). In this study, to formulate the cart pushing model, the environment of a previously validated full body gait model was modified by adding a cart segment. The accuracy of the cart and human model interaction was critical to the model computations. Since the cart motion and its orientation with respect to the human model was well controlled using the kinematic data, the cart wheel reaction forces were compared with measured vertical ground reaction forces to validate the model. Previously, De Looze et al. (1992) used a similar approach to validate their two-dimensional dynamic linked segment model.

In this study, force plates recorded the GRF at two instances: (1) when the cart wheel was moving over the force plates; (2) when the participant was stepping on the force plates (Fig. 3). The part of the GRF data in the C3D file for the cart wheels was zeroed using C3D editor. The resulting data file was used to run the cart pushing model. Vertical reaction force (Fz) for the cart wheel estimated by the model was compared with the vertical component of the GRF (Fz′) to validate the cart and human model interaction.

On average, the duration of cart wheel motion over the force plate was 0.6 ± 0.10 s. The minimum duration was nearly 0.5 s. Therefore, GRF data for 0.5 s, i.e. 50 frames (sampling frequency = 100 Hz) were used for validation. The vertical component of GRF (Fz′) recorded by the force plates was compared with the reaction force calculated by the model using root mean squared error (RMSE) estimated using the following equation (Fong et al., 2008; Plamondon et al., 2007; Wong and Wong, 2008):

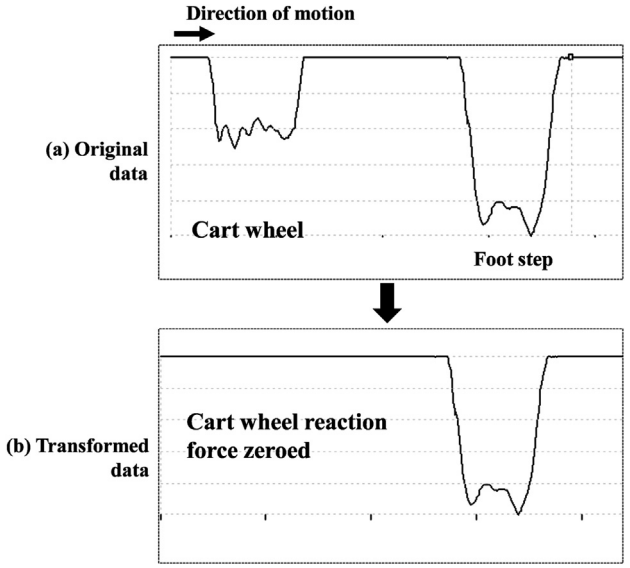

Fig. 3. (a) Vertical GRF data recorded by the force plate during cart pushing task; (b) Original data was transformed by eliminating force generated by the cart wheel.

$$\text{RMSE} = \left[\frac{1}{n}\sum_{i=1}^{n}\left(Fz_i - Fz_i'\right)^2\right]^{1/2}$$

In addition to the RMSE, the correlation coefficient (*r*) between the measured and estimated cart wheel reaction forces was calculated using the following equation:

$$r = \frac{\sum_{i=1}^{n}\left(Fz_i - \overline{Fz}\right)\left(Fz_i' - \overline{Fz'}\right)}{\sqrt{\sum_{i=1}^{n}\left(Fz_i - \overline{Fz}\right)^2}\sqrt{\sum_{i=1}^{n}\left(Fz_i' - \overline{Fz'}\right)^2}}$$

Where, *Fz* − Cart wheel reaction forces estimated by the cart pushing model;

Fz' − Vertical GFR measured by the force plates;
n − Number of samples (*n* = 50 frames), and *i* the sample number (*i* = 1, …, 50).

2.8. Statistical analysis

A two-way general linear ANOVA (analysis of variance) was performed to test the effect of cart weight and walkway gradient on the biomechanical loading of the shoulder complex and low back joints. Walkway gradient was treated as a fixed effect with three levels: (1) flat walkway with 0° gradient; (2) inclined walkway with 5° gradient; (3) inclined walkway with 10° gradient. Cart weight was also treated as a fixed factor with three levels: (1) 20 kg; (2) 30 kg; (3) 40 kg. Participants were treated as a random factor. The adequacy of the linear model was confirmed by using normal probability plots of residuals between the actual and fitted values. Significant main and/or interaction effects were further evaluated by conducting comparison between means using Tukey's Honestly Significant Difference (HSD) all-pairwise comparison test.

3. Results

3.1. Model validation

The patterns of cart wheel reaction forces predicted by the model matched closely with the experimentally measured forces (Fig. 4). The average correlation coefficient between the measured and the estimated data across all experimental conditions was 0.92 (Table 1). The average RMSE was 14.11 N, which was 3.71% of the peak vertical GRF (380 N) recorded across all experimental conditions. The RMSE up to 6% of the peak value was reported to be acceptable for validation purposes (Fong et al., 2008).

Table 1
Mean root mean squared error (RMSE) and correlation coefficient (r) between the measured and estimated cart wheel reaction forces at different experimental conditions. Numbers in the parenthesis represent one standard deviation.

Walkway gradient	Cart weight	RMSE (N)	r
0°	20 kg	11.2 (0.95)	0.95 (0.01)
0°	30 kg	11.6 (0.95)	0.95 (0.04)
0°	40 kg	13.6 (0.93)	0.93 (0.02)
5°	20 kg	13.0 (0.93)	0.93(0.04)
5°	30 kg	14.0 (0.93)	0.93(0.04)
5°	40 kg	15.4 (0.92)	0.92 (0.04)
10°	20 kg	14.9 (0.92)	0.92 (0.02)
10°	30 kg	15.5 (0.90)	0.90 (0.01)
10°	40 kg	17.4 (0.88)	0.88 (0.04)
	All	14.1 (0.92)	0.92 (0.02)

3.2. Low back loading

The main effect of the cart weight and the walkway gradient on the compression and the shear loading of L5/S1 joint was statistically significant (all $p < 0.001$) (Table 2). The peak compression and shear forces in anterioposterior and mediolateral directions increased significantly with the increase in the cart weight and the walkway gradient. The magnitude of shear forces in the mediolateral direction was minimal compared to the forces in the other two directions (compression and anterioposterior). The average of the peak forces in the mediolateral, anterioposterior, and compression directions ranged between 48 N– 142 N, 178 N–817 N, and 864 N–3245 N, respectively. The interaction effect of cart weight and walkway gradient on the peak compression and anterioposterior shear forces was statistically significant (Fig. 5) (all $p < 0.001$). A very similar increase in the loading of the L5/S1 joint in the anterioposterior and compression directions with the increase in the weight was observed at 0° and 5° gradients. But at 10° gradient, the corresponding increase in the loading was much higher (almost two times) for similar changes in the cart weight.

3.3. Shoulder joint loading

The peak loading of the shoulder joints (sternoclavicular, acromioclavicular, and glenohumeral) in three anatomical directions was significantly affected by the cart weight and the walkway gradient (all $p < 0.001$) (Table 2). For the sternoclavicular joint, the peak reaction forces in the mediolateral and inferosuperior directions were 2–3 times higher than in the anterioposterior direction. The average

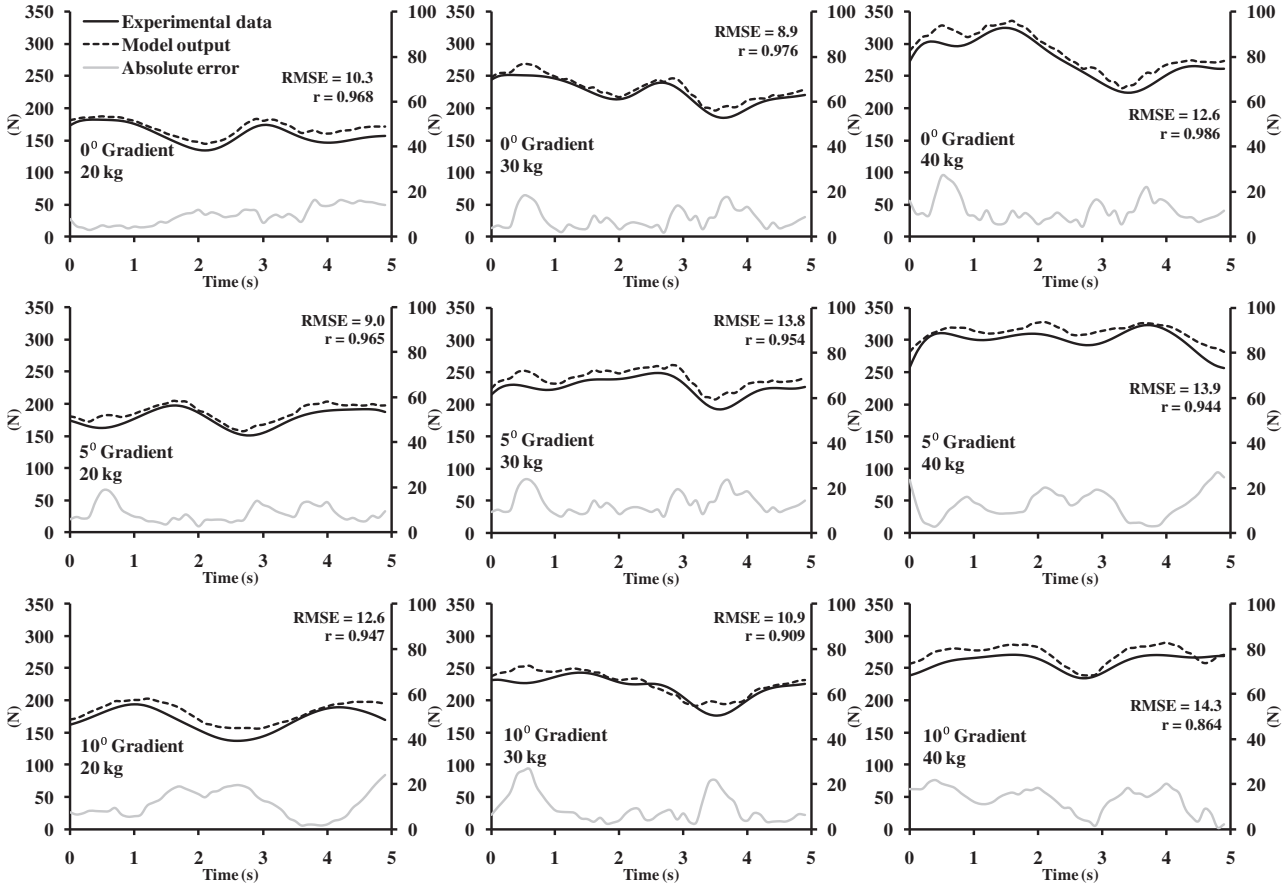

Fig. 4. Exemplar comparison of estimated and measured vertical GRF data for one of the study participants.

Table 2
Main effect of walkway gradient and cart weight on the loading of low back and shoulder joints expressed in terms of peak reaction forces (N). Numbers in the parenthesis represent one standard deviation.

Anatomical joint	Direction	Walkway gradient			*P*-value	Cart weight			*P*-value
		0°	5°	10°		20 kg	30 kg	40 kg	
Lumbosacral (L5/S1) joint	Medio-lateral (ML) shear	63.6 (34.3)	92.6 (34.3)	104.0 (37.4)	<0.001	64.1 (23.9)	80.6 (32.9)	115.0 (39.5)	<0.001
	Compression (PD)	1117.6 (305.0)	1538.6 (418.4)	2380.0 (825.0)	<0.001	1174.9 (338.8)	1666.0 (650)	2195.0 (853.0)	<0.001
	Anterior-posterior (AP) shear	239.4 (101.6)	346.9 (96.5)	569.0 (226.7)	<0.001	259.2 (89)	379.0 (165.9)	517.2 (244.0)	<0.001
Sternoclavicular (SC) joint	Medio-lateral (ML)	58.7 (22.0)	76.0 (28.6)	156.9 (70.3)	<0.001	64.6 (27.8)	107.0 (66.6)	120.0 (70.5)	<0.001
	Infero-superior (IS)	83.0 (33.2)	99.6 (35.4)	151.6 (48.2)	<0.001	76.8 (27.9)	103.5 (35.8)	153.8 (45.8)	<0.001
	Anterior-posterior (AP)	34.3 (13.9)	36.0 (9.8)	53.7 (11.6)	<0.001	34.0 (12.3)	40.5 (12.2)	49.5 (15.4)	<0.001
Acromioclavicular (AC) joint	Medio-lateral (ML)	308.9 (106.5)	337.9 (145.2)	652.9 (297.5)	<0.001	289.9 (131.5)	404.5 (196.9)	605.3 (295.7)	<0.001
	Infero-superior (IS)	396.9 (147.3)	442.4 (179.5)	782.4 (308.2)	<0.001	358.7 (141.9)	523.7 (242.3)	739.2 (294.3)	<0.001
	Anterior-posterior (AP)	238.1 (99.0)	268.2 (94.0)	499.9 (205.4)	<0.001	224.3 (100.1)	317.8 (142.0)	464.2 (207.0)	<0.001
Glenohumeral (GH) joint	Distraction (DIS)	507.5 (166.6)	669.5 (240.1)	1036.9 (301.4)	<0.001	516.5 (184.3)	720.2 (269.8)	976.7 (334.3)	<0.001
	Infero-superior (IS)	302.6 (158.2)	353.5 (202.7)	651.1 (204.3)	<0.001	282.6 (143.0)	420.0 (201.3)	604.6 (257.3)	<0.001
	Anterior-posterior (AP)	250.9 (98.7)	275.8 (96.6)	454.3 (172.9)	<0.001	210.9 (57.6)	337.7 (126.3)	432.3 (172.3)	<0.001

peak reaction forces acting at the sternoclavicular joint in the anterioposterior direction ranged between 26 and 63 N. In the mediolateral and inferosuperior directions, the corresponding values ranged between 42 and 207 N and 54 N–205 N, respectively. For the acromioclavicular joint, the average of the peak loading in the anterioposterior, mediolateral, and inferosuperior directions ranged between 169 N and 721 N, 211 N–970 N, and 263 N–1066 N, respectively. For the glenohumeral joint, the peak reaction forces acting in the distraction direction were higher than mediolateral and inferosuperior directions. The average peak reaction forces in the distraction direction ranged between 362 N and 1372 N. The corresponding values in the anterioposterior and inferosuperior directions ranged between 175 N–629 N and 185 N–867 N, respectively.

The interaction effect of cart weight and walkway gradient on the peak joint reaction forces for the sternoclavicular, acromioclavicular, and glenohumeral joints in the three anatomical directions (except anterioposterior direction for sternoclavicular joint and inferosuperior direction for glenohumeral joint) was statistically significant (Fig. 5). The increase in the gradient from 5° to 10° produced a much higher increase in the peak reaction forces compared to the increase in the gradient from 0° to 5° for the same weight conditions.

4. Discussion

Manual carts facilitate load carrying and are considered especially very useful while transferring goods on inclined walkways. This study was aimed at quantifying biomechanical loading of shoulder complex and low back joints during bimanual cart pushing tasks performed under different walkway gradient and load conditions. Peak joint reaction forces were used as the estimates of biomechanical loading of shoulder complex and low back joints.

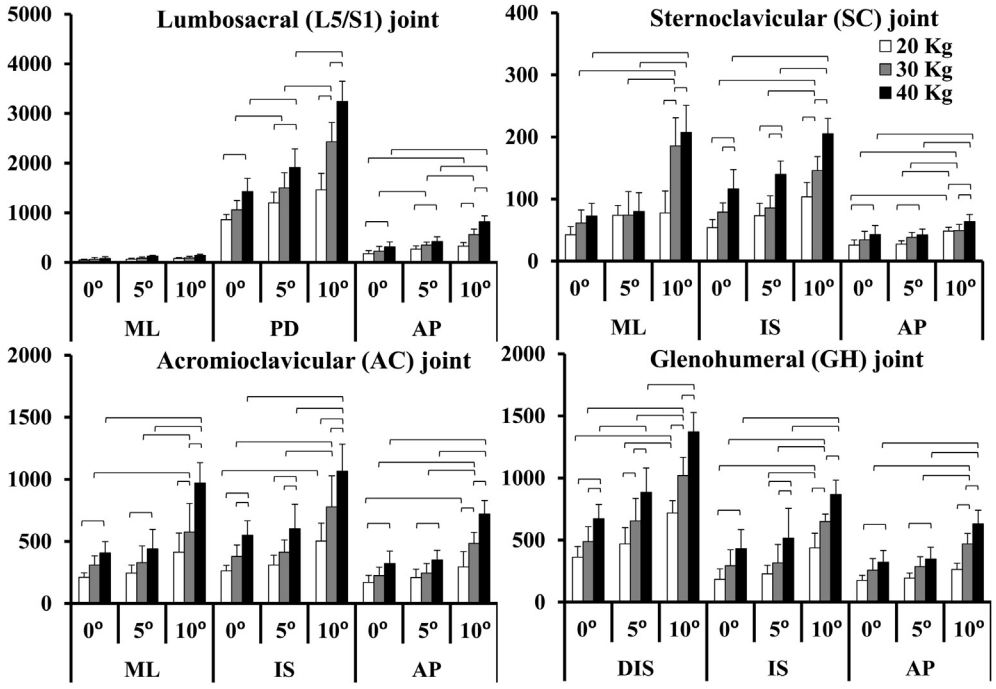

Fig. 5. Effect of weight and walkway gradient on the biomechanical loading of shoulder complex and low back joints in three anatomical directions: (1) compression (PD) or inferosuperior (IS); (2) mediolateral (ML) or distraction (DIS); (3) anterioposterior (AP) inverted brackets show results of Tukey's HSD all-pairwise comparison test. Columns marked with bracket ends are significantly different from each other. Error bar represent one standard deviation.

4.1. Low back loading

Weight of the cart and walkway gradient significantly affected the compression and shear loading in the anterioposterior directions. Relatively, a very small shear loading (<150 N) in the lateral direction was observed. A similar effect of weight and gradient on the 3D loading of low back was also reported in the previous studies (Jäger et al., 2007; Laursen and Schibye, 2002). Laursen and Schibye (2002) estimated compression and anterioposterior shear forces of up to 751 N and 952 N, and 43 N and 80 N, respectively, at the L4/L5 joint for 25 kg and 50 kg weigh conditions on a flat walkway. For 30 and 40 kg weight conditions, compression of up to 863 N and 1432 N and anterioroposterior shear loading of up to 170 and 331 N, respectively, was estimated in the present study. In a different study, Jäger et al. (2007) estimated L5/S1 compression of 800 N and 900 N, and 1200 N and 1500 N for cart weights (combined weight of cart and load) of 45 and 65 kg, on 0° and 5° inclined walkways, respectively. In the present study, L5/S1 compression of 1504 N and 1913 N, was estimated for cart weights of 42 kg and 62 kg (weight of the cart used in this study = 12 kg), respectively, on 5° inclined walkway.

Overall, the low back compression and shear loading estimated in this study were a little higher than the previous studies. The musculoskeletal model used in this study accounted for the trunk muscle co-contraction, unlike the models used in the previous studies. The level of muscle co-contraction used in the model computation affected the biomechanical estimation of joint loading. Garg and Kapellusch (2009) argued that models that do not account for the trunk muscle co-contraction underestimate spine compression forces by as much as 45% and shear forces by as much as 70%. A comparison of joint loading estimated in this study with the previous studies show that on average, compressive and anterioposterior shear forces estimated in this study were 34% and 75% higher than the previous studies.

4.2. Shoulder loading

Variation in the walkway gradient and cart weight significantly affected the reaction forces acting at the shoulder complex joints. A few previous studies have reported similar effects of weight on the net reaction moment at the glenohumeral joint during pushing and pulling exertions (Abel and Frank, 1991; De Looze et al., 2000; Laursen and Schibye, 2002; Schibye et al., 2001; Van der Woude et al., 1995). Only one previous study by Hoozemans et al. (2004) estimated reaction forces in the inferosuperior direction at the glenohumeral joint. Hoozemans et al. (2004) also derived a generalized estimating equation to assess ergonomic consequences of pushing and pulling exertions performed using a manual cart. Using this equation, a compression (inferosuperior) force of 482 N was estimated for a 40 kg weight condition on a horizontal surface. This number is somewhat different from the compression force of 430 N estimated in the present study. Hoozemans et al. (2004) used a four wheel cart and much heavier weight conditions (85, 135, and 320 kg) to derive the generalized estimating equation. The numerical difference in the joint loading estimated in the two studies may be primarily due to these differences in types of carts and the weight conditions used.

This study reported for the first time a 3D biomechanical loading of three shoulder complex joints: sternoclavicular, acromioclavicular and glenohumeral joints. While the loading of the sternoclavicular joint was found to be minimal, the reaction forces acting at the acromioclavicular joint were found to be quite high and comparable with the glenohumeral joint. A similar behavior of shoulder joints during wheelchair propulsion activities was also observed by van Drongelen et al. (2011). Anatomically, the sternocleidomastoid is the only major neck muscle that acts at the sternoclavicular joint. Upper trapezius and deltoid muscles play an important role in the stabilization of the acromioclavicular joint. Whereas, rotator cuff muscles, the supraspinatus, subscapularis, infraspinatus, and teres minor, act at the glenohumeral joint. The co-contraction of these relatively bigger and higher number of shoulder arm muscles may attribute to the higher loading of the acromioclavicular and glenohumeral joints compared to the sternoclavicular joint.

While the distraction loading was found to be higher for the glenohumeral joint than acromioclavicular joint, higher loading in the inferosuperior and anterioposterior directions were observed for the acromioclavicular joint than the glenohumeral joint. The peak distraction forces acting at the glenohumeral joints were about 1.7 times that of the acromioclavicular joint. The peak forces in the inferosuperior and anterioposterior directions at the acromioclavicular joint were about 1.3 and 1.0 times that of the glenohumeral joint. Thus, the results of this study show a similar loading pattern for the acromioclavicular and glenohumeral joints in the inferosuperior and anterioposterior directions.

4.3. Risk of WMSD

In the present study, average peak compression forces of up to 2420 N and 3222 N were observed for 30 kg and 40 kg weight conditions, respectively, on 10° walkway. These values are below the action limit of 3400 N used for the risk assessment of work-related low back disorders recommended by NIOSH (NIOSH, 1981) but are closer to/higher than the limit of 2500 N, which was chosen as the criterion for evaluating low back disc compression during trolley maneuvers by Jäger et al. (2007). In the anterioposterior direction, reaction forces greater than 500 N are considered unsafe for the loading of low back (McGill, 2007). In the present study, anterioposterior shear forces greater than 500 N were observed on the 10° ramp for the weights of 30 kg (i.e. combined weight (cart + external weight) of 42 kg) and higher. Therefore, some risk of low back injury, mainly due to the increased shear loading in the anterioposterior direction, is associated with cart pushing exertions. A similar conclusion regarding the risk of low back injury based on the comparison of compression and shear loading during cart pushing exertions was also made by Knapik and Marras (2009).

For the shoulder complex, compression forces stabilize the glenohumeral joint, whereas translational forces in mediolateral or anterioposterior direction destabilize the joint (Labriola et al., 2005). A lower ratio between translational and compression forces increases the glenohumeral joint stability and as this ratio increases, stability of the glenohumeral joint decreases (Lippitt et al., 1993). For the cart pushing tasks evaluated in this study, the translational forces acting at the glenohumeral joints in the mediolateral direction were consistently higher than the compression forces. The ratio between the translational and compression forces ranged between 1.7 and 2.0 and sufficiently high magnitude (range 650–1370 N) of mediolateral forces were observed for 40 kg weight (all gradients) and 10° gradient (weight ≥ 20 kg) conditions. High translational forces and the increased ratio between the translational and compression forces destabilize the glenohumeral joint increasing the risk of shoulder MSD with cumulative exposure.

4.4. Study limitations

A few limitations should be considered while understanding and translating findings of this study to real workplace situations. First, biomechanical loadings reported in this study are specific to the type of cart and the walkway surface used. Altered cart and

walking surfaces may result in different computational findings. Furthermore, only the sustained phase of pushing exertion was investigated because of the restriction on the capture volume associated with the motion capture system used in this study. The initial and ending phases involve different cart maneuvering tactics which may produce, possibly higher, musculoskeletal loading, especially when performed on inclined surfaces (Bennett et al., 2008). Finally, participation in this study was voluntary and the participant pool was limited to university-aged students with little manual materials handling experience. Furthermore, only male subjects were tested in this study. Experienced workers as well as females may use different force exertion strategies. Future studies should look at larger, more diverse working conditions characterized by different work-surfaces, cart designs, populations with manual materials handling experience, and both genders to determine how well the trends observed in the current study could be applied to the working conditions and population.

4.5. Conclusion

In this study, biomechanical loading of three shoulder complex joints, in addition to the low back joint were estimated during cart pushing tasks using a comprehensive full body musculoskeletal model. Cart weight and walkway gradient appeared to affect the mechanical load on the shoulder complex and low back joints. While the compression loading was low, shear loading may increase the risk of low back WMSDs. Among the shoulder complex joints, biomechanical loading of the acromioclavicular joint was found to be high and quite comparable with the glenohumeral joints. Therefore, ergonomic evaluation of cart pushing tasks should consider mechanical loading of the acromioclavicular joints in addition to the glenohumeral and low back joints.

Acknowledgments

The authors thank Chris Moore for his assistance in developing and constructing the experimental set up. The authors also sincerely thank the anonymous reviewers for their invaluable comments to improve this article. Disclaimers: The findings and conclusions in this report are those of the authors and do not necessarily represent the views of the National Institute for Occupational Safety and Health. Mention of company names or products does not imply endorsement by the National Institute for Occupational Safety and Health.

References

Abel, E., Frank, T., 1991. The design of attendant propelled wheelchairs. Prosthetics and Orthotics International 15, 38.
AnyBody Modeling System, 2012. AnyBody Tutorials. Available at: http://www.anybodytech.com/fileadmin/AnyBody/Docs/Tutorials/main/main.html.
AnyBody Technology, 2011. The AnyScript Model Repository.
Bennett, A., Desai, S., Todd, A., Freeland, H., 2008. The effects of load and gradient on hand force responses during dynamic pushing and pulling tasks. Ergonomics SA: Journal of the Ergonomics Society of South Africa 20, 3–15.
Bureau of Labor Statistics, 2010. Nonfatal Occupational Injuries and Illnesses Requiring Days Away From Work, 2009. U.S. Bureau of Labor Statistics, Washington, DC.
Damsgaard, M., Rasmussen, J., Christensen, S.T., Surma, E., de Zee, M., 2006. Analysis of musculoskeletal systems in the AnyBody Modeling System. Simulation Modelling Practice and Theory 14, 1100–1111.
De Looze, M., Kingma, I., Bussmann, J., Toussaint, H., 1992. Validation of a dynamic linked segment model to calculate joint moments in lifting. Clinical Biomechanics 7, 161–169.
De Looze, M., Van Greuningen, K., Rebel, J., Kingma, I., Kuijer, P., 2000. Force direction and physical load in dynamic pushing and pulling. Ergonomics 43, 377–390.
de Zee, M., Rasmussen, J., 2009. Using musculoskeletal modeling for estimating the most important muscular output-force. Modelling the Physiological Human, 62–70.
Dubowsky, S., Rasmussen, J., Sisto, S., Langrana, N., 2008. Validation of a musculoskeletal model of wheelchair propulsion and its application to minimizing shoulder joint forces. Journal of Biomechanics 41, 2981–2988.
Dunning, K.K., Davis, K.G., Cook, C., Kotowski, S.E., Hamrick, C., Jewell, G., Lockey, J., 2010. Costs by industry and diagnosis among musculoskeletal claims in a state workers compensation system: 1999–2004. American Journal of Industrial Medicine 53, 276–284.
Fong, D.T.P., Chan, Y.Y., Hong, Y., Yung, P.S.H., Fung, K.Y., Chan, K.M., 2008. A three-pressure-sensor (3PS) system for monitoring ankle supination torque during sport motions. Journal of Biomechanics 41, 2562–2566.
Garg, A., Kapellusch, J., 2009. Applications of biomechanics for prevention of work-related musculoskeletal disorders. Ergonomics 52, 36–59.
Glitsch, U., Ottersbach, H., Ellegast, R., Schaub, K., Franz, G., Jäger, M., 2007. Physical workload of flight attendants when pushing and pulling trolleys aboard aircraft. International Journal of Industrial Ergonomics 37, 845–854.
Grujicic, M., Pandurangan, B., Xie, X., Gramopadhye, A., Wagner, D., Ozen, M., 2010. Musculoskeletal computational analysis of the influence of car-seat design/adjustments on long-distance driving fatigue. International Journal of Industrial Ergonomics 40, 345–355.
Hoozemans, M., Kuijer, P., Kingma, I., van Dieën, J., de Vries, W., van der Woude, L., Dirk, J., van der Beek, A., Frings-Dresen, M., 2004. Mechanical loading of the low back and shoulders during pushing and pulling activities. Ergonomics 47, 1–18.
Hoozemans, M., van der Beek, A., Frings-Dresen, M., Van der Woude, L., Van Dijk, F., 2002a. Low-back and shoulder complaints among workers with pushing and pulling tasks. Scandinavian Journal of Work, Environment & Health 28, 293–303.
Hoozemans, M., Van der Beek, A., Frings-Dresen, M., Van der Woude, L., Van Dijk, F., 2002b. Pushing and pulling in association with low back and shoulder complaints. Occupational and Environmental Medicine 59, 696–702.
Hoozemans, M., van der Beek, A., Frings-Dresen, M., van Dijk, F., van der Woude, L., 1998. Pushing and pulling in relation to musculoskeletal disorders: a review of risk factors. Ergonomics 41, 757–781.
Hughes, R.E., Silverstein, B.A., Evanoff, B.A., 1997. Risk factors for work related musculoskeletal disorders in an aluminum smelter. American Journal of Industrial Medicine 32, 66–75.
Jäger, M., Sawatzki, K., Glitsch, U., Ellegast, R., Ottersbach, H.J., Schaub, K., Franz, G., Luttmann, A., 2007. Load on the lumbar spine of flight attendants during pushing and pulling trolleys aboard aircraft. International Journal of Industrial Ergonomics 37, 863–876.
Knapik, G., Marras, W., 2009. Spine loading at different lumbar levels during pushing and pulling. Ergonomics 52, 60–70.
Labriola, J.E., Lee, T.Q., Debski, R.E., McMahon, P.J., 2005. Stability and instability of the glenohumeral joint: the role of shoulder muscles. Journal of Shoulder and Elbow Surgery 14, S32–S38.
Laursen, B., Schibye, B., 2002. The effect of different surfaces on biomechanical loading of shoulder and lumbar spine during pushing and pulling of two-wheeled containers. Applied Ergonomics 33, 167–174.
Lee, P., Granata, K., 2006. Interface stability influences torso muscle recruitment and spinal load during pushing tasks. Ergonomics 49, 235–248.
Lippitt, S.B., Vanderhooft, J.E., Harris, S.L., Sidles, J.A., Harryman, D.T., Matsen, F.A., 1993. Glenohumeral stability from concavity-compression: a quantitative analysis. Journal of Shoulder and Elbow Surgery 2, 27–35.
Manders, C., New, A., Rasmussen, J., 2008. Validation of musculoskeletal gait simulation for use in investigation of total hip replacement. Journal of Biomechanics 41, 488.
McGill, S., 2007. Low Back Disorders: Evidence-based Prevention and Rehabilitation. Human Kinetics Publishers, Champaign, IL.
NIOSH, 1981. Work Practices Guide for Manual Lifting. Tech. Report No. 81-122. U.S. Dept. of Health and Human Services (NIOSH), Cincinnati, OH.
OSHA, 2005. 29 CFR 1910, Subpart D – Walking-Working Surfaces.
Plamondon, A., Delisle, A., Larue, C., Brouillette, D., McFadden, D., Desjardins, P., Lariviere, C., 2007. Evaluation of a hybrid system for three-dimensional measurement of trunk posture in motion. Applied Ergonomics 38, 697–712.
Rasmussen, J., Damsgaard, M., Voigt, M., 2001. Muscle recruitment by the min/max criterion – a comparative numerical study. Journal of Biomechanics 34, 409–415.
Rasmussen, J., de Zee, M., Trholm, S., Damsgaard, M., 2007. Comparison of a musculoskeletal shoulder model with in-vivo joint forces. Journal of Biomechanics 40, 67.
Schibye, B., Søgaard, K., Martinsen, D., Klausen, K., 2001. Mechanical load on the low back and shoulders during pushing and pulling of two-wheeled waste containers compared with lifting and carrying of bags and bins. Clinical Biomechanics 16, 549–559.
Smedley, J., Inskip, H., Trevelyan, F., Buckle, P., Cooper, C., Coggon, D., 2003. Risk factors for incident neck and shoulder pain in hospital nurses. Occupational and Environmental Medicine 60, 864.
Smith, J., Woldstad, J., Patterson, P., 2009. Ergonomics of manual materials handling. In: Kutz, M. (Ed.), Environmentally Conscious Materials Handling. John Wiley & Sons, Inc., Hoboken, NJ.
Snook, S., 1978. The design of manual handling tasks. Ergonomics 21, 963–985.
van der Beek, A., Frings-Dresen, M., van Dijk, F., Kemper, H., Meijman, T., 1993. Loading and unloading by lorry drivers and musculoskeletal complaints. International Journal of Industrial Ergonomics 12, 13–23.

van der Beek, A., Hoozemans, M., Frings-Dresen, M., Burdorf, A., 1999. Assessment of exposure to pushing and pulling in epidemiological field studies: an overview of methods, exposure measures, and measurement strategies. International Journal of Industrial Ergonomics 24, 417–429.

Van der Woude, L., Van Konlngsbruggen, C., Kroes, A., Kingma, I., 1995. Effect of push handle height on net moments and forces on the musculoskeletal system during standardized wheelchair pushing tasks. Prosthetics and Orthotics International 19, 188–201.

van Drongelen, S., van der Woude, L., Veeger, H., 2011. Load on the shoulder complex during wheelchair propulsion and weight relief lifting. Clinical Biomechanics 26, 452–457.

Vicon Plug in Gait Manual, 2003. Oxford Metrics Ltd, Oxford UK.

Waters, T., Putz-Anderson, V., Garg, A., Fine, L., 1993. Revised NIOSH equation for the design and evaluation of manual lifting tasks. Ergonomics 36, 749–776.

Wong, W.Y., Wong, M.S., 2008. Trunk posture monitoring with inertial sensors. European Spine Journal 17, 743–753.

Wu, J., An, K., Cutlip, R., Krajnak, K., Welcome, D., Dong, R., 2008. Analysis of musculoskeletal loading in an index finger during tapping. Journal of Biomechanics 41, 668–676.

Wu, J., Chiou, S., Pan, C., 2009. Analysis of musculoskeletal loadings in lower limbs during stilts walking in occupational activity. Annals of Biomedical Engineering 37, 1177–1189.